

Investigation of Anomalous Estimates of Tensor-Derived Quantities in Diffusion Tensor Imaging

Cheng Guan Koay,^{*1,2} John D. Carew,³ Andrew L. Alexander,⁴ Peter J. Basser,² and M. Elizabeth Meyerand⁴

The diffusion tensor is typically assumed to be positive definite. However, noise in the measurements may cause the eigenvalues of the tensor estimate to be negative, thereby violating this assumption. Negative eigenvalues in diffusion tensor imaging (DTI) data occur predominately in regions of high anisotropy and may cause the fractional anisotropy (FA) to exceed unity. Two constrained least squares methods for eliminating negative eigenvalues are explored. These methods, the constrained linear least squares method (CLLS) and the constrained nonlinear least squares method (CNLS), are compared with other commonly used algebraic constrained methods. The CLLS tensor estimator can be shown to be equivalent to the linear least squares (LLS) tensor estimator when the LLS tensor estimate is positive definite. Similarly, the CNLS tensor estimator can be shown to be equivalent to the nonlinear least squares (NLS) tensor estimator when the NLS tensor estimate is positive definite. The constrained least squares methods for eliminating negative eigenvalues are evaluated with both simulations and in vivo human brain DTI data. Simulation results show that the CNLS method is, in terms of mean squared error for estimating trace and FA, the most effective method for correcting negative eigenvalues. Magn Reson Med 55:930–936, 2006. Published 2006 Wiley-Liss, Inc.†

Key words: diffusion tensor imaging; negative diffusivity; fractional anisotropy; constrained optimization; diffusion tensor estimation

Water diffusion as measured by diffusion tensor imaging (DTI) is a unique noninvasive approach to investigate and characterize the microstructural properties of biologic tissues (1–4). Several rotationally invariant scalar measures have been constructed to extract important information from the diffusion tensors (3,5,6). The most common tensor-derived scalar measures are the fractional anisotropy (FA) and the trace of the diffusion tensor (6,7). Interpretations and comparisons of these scalar measures are influenced by the accuracy of the diffusion tensor estimates.

Measurement noise can cause errors in the diffusion tensor estimates. If the measurement errors from noise, physiologic fluctuations, and image misregistration are large enough, the diffusion tensor estimate may not be positive definite. Further, these measurement errors may cause the FA, which in theory should range from zero to 1, to exceed 1, particularly in regions with high diffusion anisotropy such as the corpus callosum and the corticospinal tract.

In the present study, we describe two constrained least squares methods [the constrained linear least squares method (CLLS) and the constrained nonlinear least squares method (CNLS)] for eliminating the negative eigenvalues. These constrained methods can be recast as the unconstrained optimization methods through the Cholesky parametrization for the diffusion tensor; the Cholesky parametrization is one of the unconstrained parametrizations for variance–covariance matrices discussed by Pinheiro and Bates (8). Within the context of DTI, the Cholesky parametrization has been used in combination with an adaptive smoothing technique by Wang et al. (9). However, this previous study did not specifically investigate the effect of constraint satisfaction on the quantitative accuracy of the tensor-derived quantities. In this study, the CLLS and CNLS methods were evaluated and compared with other algebraic constrained methods using both measured human brain DTI data and Monte Carlo simulations. Three algebraic constrained methods are explored in this work. The first algebraic constrained method is a pre-estimation method that replaces the measured diffusion-weighted signals that are greater than the reference (measured non-diffusion-weighted) signal with the reference signal. The second method is a postestimation method that replaces the negative eigenvalues with zero. The last method is also a postestimation method that replaces the negative eigenvalues with their absolute values.

Based on the simulation studies, the nonlinear methods (nonlinear least squares (NLS) and CNLS) have lower mean squared errors in estimating the trace and FA than the linear methods (linear least squares (LLS) and CLLS) and other algebraic constrained methods listed above. Further, the CNLS method has lower mean squared errors in estimating the trace and FA than the NLS method.

THEORY AND METHODS

In a DT-MRI experiment, the measured signal in a single voxel may be modeled as (1,2,10)

$$S = S_0 \exp(-bg^T Dg), \quad [1]$$

where the measured signal is a function of the diffusion encoding unit vector g , the reference signal S_0 , and the

¹Department of Physics, University of Wisconsin–Madison, Madison, Wisconsin, USA.

²Laboratory of Integrative & Medical Biophysics, National Institutes of Health, Bethesda, Maryland, USA.

³Department of Statistics, University of Wisconsin–Madison, Madison, Wisconsin, USA.

⁴Department of Medical Physics, University of Wisconsin–Madison, Madison, Wisconsin, USA.

Grant numbers: MH062015 and EB002012; Grant sponsor: NIH; Grant number: EY07119.

*Correspondence to: Cheng Guan Koay, STBB/LIMB/NICHD, National Institutes of Health, Building 13, Room 3W16, 13 South Drive, Bethesda, MD 20892, USA. E-mail: guankoac@mail.nih.gov

Received 2 December 2004; revised 9 November 2005; accepted 10 November 2005

DOI 10.1002/mrm.20832

Published online 8 March 2006 in Wiley InterScience (www.interscience.wiley.com).

diffusion weighting b . The superscript T denotes vector transpose ($\mathbf{g} = [g_x \ g_y \ g_z]^T$ being a column vector). The diffusion tensor \mathbf{D} is a 3 by 3 symmetric positive definite tensor.

At a particular pixel location, let S_i and \mathbf{g}_i (with $i = 1, \dots, N$) be the measured diffusion-weighted signal and the diffusion encoding unit vector in the i th diffusion gradient direction, respectively. The number of encoding directions is N . Rewriting Eq. [1] for each diffusion-weighted signal, we have

$$S_i = S_0 \exp(-b \mathbf{g}_i^T \mathbf{D} \mathbf{g}_i), \quad \text{with } i = 1, \dots, N. \quad [2]$$

For a measured set of S_i values, there are several approaches for estimating the diffusion tensor. They are briefly reviewed here.

A solution to Eq. [2] may be obtained by using NLS method with the following objective function to be minimized:

$$f_{\text{NLS}}(\boldsymbol{\beta}) = \frac{1}{2} \sum_{i=1}^N \left(S_i - S_0 \exp \left[\sum_{j=1}^6 X_{ij} \beta_j \right] \right)^2, \quad [3]$$

where

$$\boldsymbol{\beta} = [D_{xx} \ D_{yy} \ D_{zz} \ D_{xy} \ D_{yz} \ D_{xz}]^T \quad [4]$$

is a vector representation of the diffusion tensor and

$$\mathbf{X} = -b \begin{pmatrix} g_{1x}^2 & g_{1y}^2 & g_{1z}^2 & 2g_{1x}g_{1y} & 2g_{1y}g_{1z} & 2g_{1x}g_{1z} \\ \vdots & \vdots & \vdots & \vdots & \vdots & \vdots \\ g_{Nx}^2 & g_{Ny}^2 & g_{Nz}^2 & 2g_{Nx}g_{Ny} & 2g_{Ny}g_{Nz} & 2g_{Nx}g_{Nz} \end{pmatrix} \quad [5]$$

is the encoding gradient design matrix. General minimization routines can be used to solve the NLS problem in Eq. [3] but most routines need a good starting value (guess solution). Fortunately, one of the advantages of a transformably linear model is the ease of finding a starting value (11). Since the DTI model is a transformably linear model, dividing both sides of Eq. [2] by the reference signal S_0 and then taking the natural log on both sides of this equation yields a linearized equation of the following form:

$$\ln(S_i/S_0) = -b \mathbf{g}_i^T \mathbf{D} \mathbf{g}_i, \quad \text{with } i = 1, \dots, N. \quad [6]$$

In the context of DTI, the starting value can be obtained by working with the linearized equation shown in Eq. [6]. Working with Eq. [6] leads to the LLS problem with the following objective function to be minimized:

$$f_{\text{LLS}}(\boldsymbol{\beta}) = \frac{1}{2} \|\mathbf{y} - \mathbf{X}\boldsymbol{\beta}\|^2 = \frac{1}{2} \sum_{i=1}^N \left(y_i - \sum_{j=1}^6 X_{ij} \beta_j \right)^2, \quad [7]$$

where

$$\mathbf{y} = [\ln(S_1/S_0) \ \dots \ \ln(S_N/S_0)]^T.$$

The solution to the LLS problem may also be written explicitly as

$$\hat{\boldsymbol{\beta}} = [\mathbf{X}^T \mathbf{X}]^{-1} \mathbf{X}^T \mathbf{y} = \mathbf{X}^+ \mathbf{y}, \quad [8]$$

where $\hat{\boldsymbol{\beta}}$ denotes the linear squares estimator of $\boldsymbol{\beta}$ and \mathbf{X}^+ denotes the pseudoinverse of \mathbf{X} (12). The LLS method is mostly widely used, although the NLS method has been applied as well. The theoretical analysis of the effects of noise on the linearized equation, Eq. [7], was explored by Anderson (13). The work of Papadakis et al. (14) focused on the nonlinear equation, Eq. [3], in constructing a new measure of curve fitting error. Outlier rejection methods working with both equations, Eqs. [3] and [7], were used by Mangin et al. (15) and Chang et al. (16).

Negative Eigenvalue Problems and Constrained Solutions

To model a diffusion process, the diffusion tensor is assumed to be symmetric positive definite (PD)—in other words the eigenvalues of the diffusion tensor estimate must be real and positive. The real eigenvalue condition on the diffusion tensor estimate is automatically satisfied based on the structure of the design matrix, \mathbf{X} , in Eq. [5]. However, the positive eigenvalue condition may not be satisfied and enforcing the condition requires more elaborate constraints not on the design matrix \mathbf{X} but on the diffusion tensor parameter vector, $\boldsymbol{\beta}$. One such approach is known as the Cholesky parametrization (8). The Cholesky parametrization states that if \mathbf{R} is an upper triangular matrix with nonzero diagonal elements

$$\mathbf{R} = \begin{pmatrix} R_0 & R_3 & R_5 \\ 0 & R_1 & R_4 \\ 0 & 0 & R_2 \end{pmatrix}, \quad [9]$$

and $\mathbf{D} = \mathbf{R}^T \mathbf{R}$, then \mathbf{D} will be a symmetric positive definite matrix. Consequently, the diffusion tensor parameter vector $\boldsymbol{\beta}$ may be written as a vector-valued function of

$$\boldsymbol{\rho} = [R_0 \ R_1 \ R_2 \ R_3 \ R_4 \ R_5]^T;$$

$$\boldsymbol{\beta}(\boldsymbol{\rho}) = [R_0^2, R_1^2 + R_3^2, R_2^2 + R_4^2 + R_5^2, R_0 R_3, R_1 R_4 + R_3 R_5, R_0 R_5]^T. \quad [10]$$

Rewriting Eqs. [3] and [7] in terms of $\boldsymbol{\rho}$, we have two objective functions,

$$f_{\text{CNLS}}(\boldsymbol{\rho}) = \frac{1}{2} \sum_{i=1}^N \left(S_i - S_0 \exp \left[\sum_{j=1}^6 X_{ij} \beta_j(\boldsymbol{\rho}) \right] \right)^2 \quad [11]$$

for the CNLS estimation and

$$f_{\text{CLLS}}(\boldsymbol{\rho}) = \frac{1}{2} \sum_{i=1}^N \left(y_i - \sum_{j=1}^6 X_{ij} \beta_j(\boldsymbol{\rho}) \right)^2 \quad [12]$$

for the CLLS estimation. Any unconstrained optimization routine may be used to solve Eqs. [11] and [12] (18).

The equivalence between the LLS estimate and the CLLS estimate, when the LLS estimate is positive definite, is established in the Appendix. Similarly, the CNLS estimate may be shown to be equivalent to the NLS estimate when the NLS estimate is positive definite. Definiteness of a tensor estimate can be determined by a condition that does not require tensor diagonalization. That is, \mathbf{D} is positive definite if and only if the determinants of all the leading principal submatrices of \mathbf{D} are positive (17),

$$D_{xx} > 0, \quad (D_{xx}D_{yy} - D_{xy}^2) > 0, \quad \text{and} \quad \det(\mathbf{D}) > 0, \quad [13]$$

where $\det(\mathbf{D})$ denotes the matrix determinant of \mathbf{D} .

Given the conditions in Eq. [13] and the equivalence conditions above, we know the exact situation when the constrained methods (CLLS and CNLS) are needed. This insight will facilitate efficient DTI data processing because it is computationally more efficient to employ the unconstrained methods (LLS or NLS) than the constrained methods (CLLS or CNLS). Particularly, the LLS method is more efficient than the CLLS method by at least a factor of 2 or more, if one takes into account the initialization needed for the CLLS method and the number of iterations needed to achieve convergence.

Fractional Anisotropy Anomaly

The fractional anisotropy anomaly refers to the situation when the FA value is greater than unity. The upper bound for the FA value is often assumed to be unity; this assumption is only true if the diffusion tensor estimate is positive definite. A commonly used formula for FA is written as (6,20)

$$FA = \frac{\sqrt{3((\lambda_1 - \langle \lambda \rangle)^2 + (\lambda_2 - \langle \lambda \rangle)^2 + (\lambda_3 - \langle \lambda \rangle)^2)}}{\sqrt{2(\lambda_1^2 + \lambda_2^2 + \lambda_3^2)}} \\ = \sqrt{\frac{3}{2} \left[1 - \frac{1}{3} \frac{\text{Tr}(\mathbf{D})^2}{\text{Tr}(\mathbf{D}^2)} \right]}, \quad [14]$$

where λ_i with $i = 1, 2, 3$ are the eigenvalues of the diffusion tensor, $\langle \lambda \rangle$ is the mean value of these eigenvalues, and the symbol Tr denotes the trace operation.

According to Eq. [14], FA greater than unity is equivalent to the condition

$$\lambda_1\lambda_2 + \lambda_1\lambda_3 + \lambda_2\lambda_3 < 0. \quad [15]$$

Equation [15] implies that there is at least one but no more than two negative eigenvalues in the diffusion tensor estimate; however, the converse is not generally true because the validity of Eq. [15] depends on the size of the negative eigenvalues.

Simulations

Monte Carlo simulations (similar to Pierpaoli et al. (6)) were performed to investigate the effects of noise on the trace and FA estimates and to evaluate the performance of various estimators in terms of the mean squared errors in estimating both FA and trace. The frequencies of non-positive definite (nonPD) tensor estimates from both LLS

and NLS algorithms as a function of SNR and FA were investigated.

In the mean squared error analysis, the least squares methods (LLS, NLS, CLLS, and CNLS) were evaluated and compared with the other constrained algebraic methods. Listed here are three algebraic constrained methods considered in this article.

LLS II

This is a pre-estimation method that replaces the measured diffusion-weighted signals that are greater than the reference signal with the reference signal itself. The LLS method will be used to estimate the diffusion tensor based on the modified measured diffusion-weighted signals.

ZERO

This is a postestimation method that replaces the negative eigenvalues with zero.

ABS

This is also a postestimation method that replaces the negative eigenvalues with their absolute values.

As mentioned earlier, the only difference between the LLS estimate and the CLLS estimate (or between the NLS estimate and the CNLS estimate) lies in the case when the LLS estimate (or the NLS estimate) is not positive definite. Furthermore, as FA increases, so does the frequency of nonPD tensors, making simulations with high FA values (>0.4) and low SNR levels (<50) more appropriate in investigating this difference. Particularly, three cylindrically symmetric tensors of FA 0.358, 0.864, and 0.962 were selected in the Results. The numerical values of these simulated tensors are $\beta = \{1.045\text{e-}3, 5.721\text{e-}4, 5.721\text{e-}4, 0, 0, 0\}, \{1.758\text{e-}3, 2.158\text{e-}4, 2.158\text{e-}4, 0, 0, 0\}$, and $\{2.041\text{e-}3, 7.433\text{e-}5, 7.433\text{e-}5, 0, 0, 0\}$ mm²/s. These three FA values were selected to show both the effects of nonPD tensors on the FA and trace estimates and the equivalence of various methods of estimation. A low FA value (0.358) was chosen to show the equivalence of various methods discussed above, i.e., between NLS and CNLS and between CLLS and LLS. Two relatively high FA values (0.864 and 0.962) were chosen to show the effects of nonPD tensor estimates on the estimated values of FA and trace. A single diffusion weighting of 1000 s/mm² was used in the simulation studies because the effects of the noise floor on tensor estimates at this diffusion weighting are minimal and less critical. The effects of the noise floor on tensor estimates have been investigated by Jones and Bassar (19).

Human Brain Imaging Experiment

DT-MRI studies were performed on a human volunteer using a Signa 3.0 T scanner (General Electric Medical Systems, Milwaukee, WI, USA). Informed consent was obtained from the subject in accordance with the guidelines of our institutional review board for human subject studies. A cardiac-gated, pulsed-gradient, spin echo with single-shot EPI readout was used for DW imaging. The set of encoding directions used in this experiment has 12 directions. The width, spacing, and amplitude of the dif-

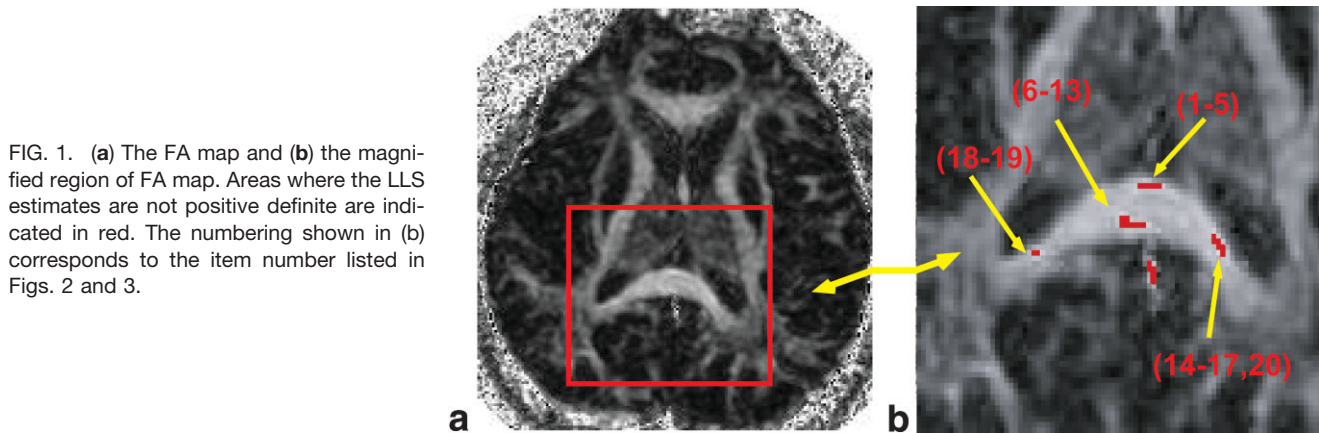


FIG. 1. (a) The FA map and (b) the magnified region of FA map. Areas where the LLS estimates are not positive definite are indicated in red. The numbering shown in (b) corresponds to the item number listed in Figs. 2 and 3.

fusion gradient pulses were 25 ms, 36 ms, and 30 mT/m yielding a b value of 1113.91 s/mm^2 . Other imaging parameters were $TR = 4.68 \text{ s}$, $TE = 79.5 \text{ ms}$, field of view = $240 \times 240 \text{ mm}^2$, number of slices = 5, slice thickness = 4 mm, and each DW and nonDW image is an average image of three magnitude images. The signal-to-noise ratio ($SNR = \text{signal amplitude}/SD \text{ of noise}$) taken from the nonDW image was approximately 19.19 ± 6.85 as determined from several patches of small ROIs of the brain.

RESULTS

Figure 1a shows an FA map computed based on the LLS method and Fig. 1b shows a magnified image of the FA map with colored areas indicating the nonPD LLS tensor estimates. The eigenvalues of these nonPD LLS tensor estimates are shown in Fig. 2. The item numbers shown in Figs. 2 and 3 correspond to the voxel numbers indicated in Fig. 1b. Various estimation methods (LLS II, CLLS, NLS, and CNLS) are also used in calculating the eigenvalue estimates shown in Fig. 2. Figure 2 shows that some of the NLS estimates (Item 5–13 in Fig. 2) are positive definite even though the corresponding LLS estimates are not. The FA values and the trace values are shown in Figs. 3a and b, respectively. The CNLS estimates and the NLS estimates are observed to be equivalent when the NLS estimates are positive definite (Item 5–13 in Figs. 2 and 3). This observation agrees with the equivalence condition on the NLS and CNLS tensor estimates mentioned in Section 2.1.

Figure 4 shows the frequency of nonPD tensor estimates for simulations as a function of SNR and FA for both the LLS method and the NLS method. This plot clearly illustrates that the NLS method has much lower likelihood of nonPD tensor estimation. This result is similar to the observation made on the human brain data in Fig. 2. The simulated effects of the algorithms on the estimated values of FA and trace as a function of SNR are shown in Figs. 5 and 6, respectively. Based on the results shown in Figs. 5 and 6, the CNLS method has the lowest mean squared errors in estimating either trace or FA.

DISCUSSION

The aim of this study was to demonstrate the effects of non-positive definite tensors on the quantitative diffusion

tensor measures (FA and trace) and to explore various methods for solving this problem. All methods except the LLS II were effective in eliminating negative eigenvalues, although they were not equivalent in terms of accuracy and stability. The constrained least squares methods (CLLS and CNLS) provide a simple generalization to the usual least squares methods used in DTI so that the negative eigenvalue problem can be solved objectively rather than using ad hoc methods to correct this problem. The constrained least squares methods (CLLS and CNLS) use the Cholesky parametrization, which constrains the estimated tensors to be positive definite.

The incidence of nonPD diffusion tensors is ultimately linked to the diffusion anisotropy, diffusion weighting, and SNR. From Fig. 4, it is clear that the rate of nonPD tensor estimates is much lower for NLS relative to LLS. This observation coupled with the recent study by Jones and Basser (19), which demonstrated that NLS methods produce more accurate estimates than LLS methods, provides converging evidence that NLS methods are better for diffusion tensor estimation.

According to Fig. 2, both CLLS and CNLS result in minor eigenvalue estimates that are close to zero when the respective LLS and NLS algorithms produce negative eigenvalues. Note that this is similar to the ZERO algorithm, except that the CLLS and CNLS adjust the other eigenvalues as well. Figures 5 and 6 show that CLLS has similar yet slightly more accurate behavior relative to the ZERO method. The CNLS appears to be the most accurate and stable method, especially at low SNR. However, it should be noted that for all algorithms the SNR is the main limiting factor in terms of accuracy and stability and the CNLS does not correct for all the problems related to low SNR. Since the nonPD cases are caused by errors in the minor eigenvalue estimates, the algorithms do not significantly alter major eigenvector direction. The maximum difference in the vector direction between algorithms was 2.3° (not shown).

The focus of this study was to investigate various post-processing methods of solving the negative eigenvalue problem with the assumption that Johnson RF (Gaussian) noise is the principal factor contributing to the problem. If this assumption is valid, then it can be concluded that the CNLS method is the most effective method among those considered here in treating the negative eigenvalue prob-

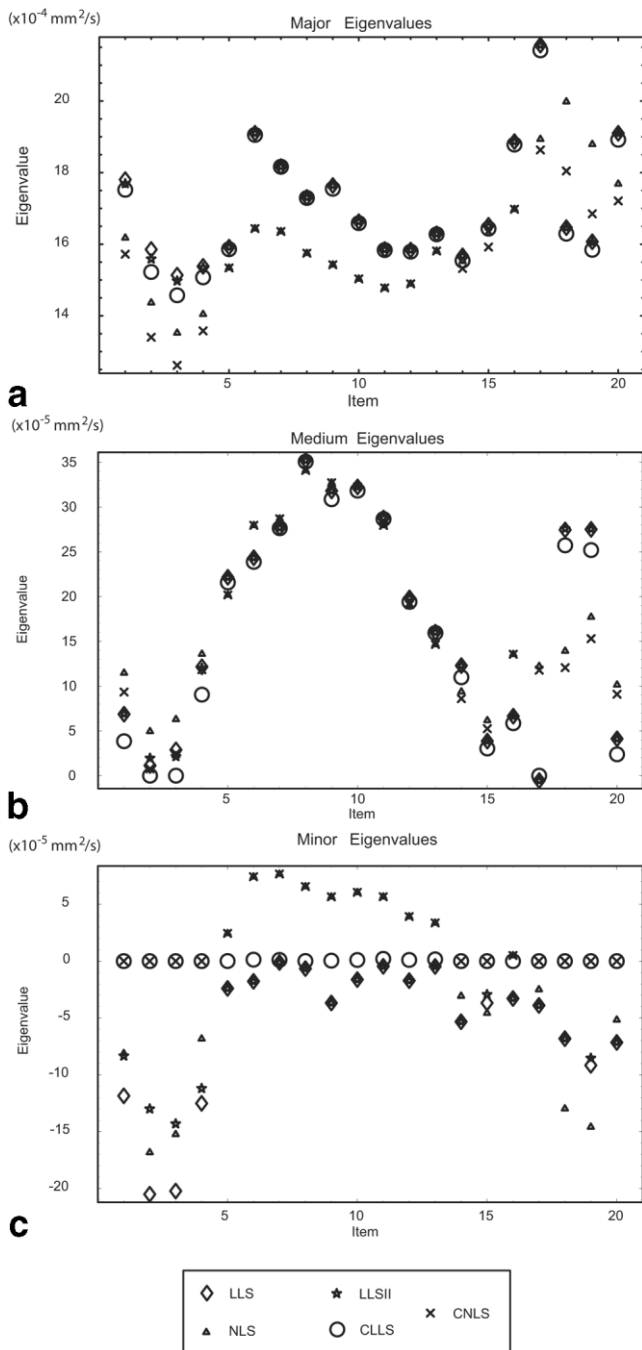


FIG. 2. The eigenvalue estimates of the nonPD tensors of Fig. 1b. Several methods of tensor estimation are used in computing the eigenvalue estimates. These methods are LLS, NLS, LLSII, CLLS, and CNLS. The plots of major, medium, and minor eigenvalue estimates are shown in (a), (b), and (c), respectively.

lem in the sense that it has the lowest mean squared errors in estimating FA and trace. Nevertheless, further studies are needed to investigate other factors encountered in a biologic or clinical setting including partial volume effects, physiologic noise, susceptibility, DW image misregistration, and hardware errors.

CONCLUSION

The NLS method resulted in fewer nonpositive definite tensors than the linear least squares method, and the constrained nonlinear least squares (CNLS) method demonstrated the lowest mean squared errors in estimating FA and trace.

APPENDIX

The solution obtained by the SVD method is equivalent to that of the CLLS method when the tensor matrix D is positive definite.

Rewriting Eq. [12] as

$$f(\boldsymbol{\beta}(\boldsymbol{\rho})) = \frac{1}{2} \| \mathbf{y} - \mathbf{X} \cdot \boldsymbol{\beta}(\boldsymbol{\rho}) \|^2, \quad [A1]$$

we can think of transforming the constrained case to the unconstrained case as a change of variables. Using the basic chain rule and setting the derivative of the function with respect to ρ_i for all i to zero we have

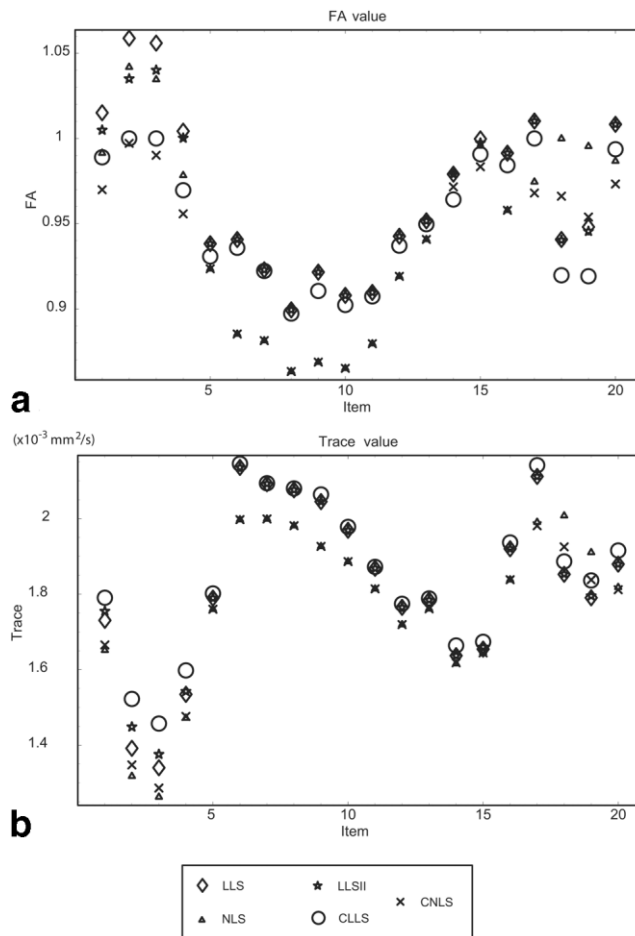


FIG. 3. The estimated FA and trace values of the nonPD tensors of Fig. 1b. (a) The plot of the estimated FA. (b) The plot of the estimated trace.

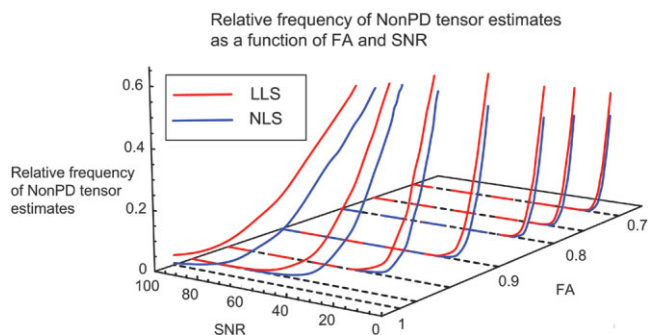


FIG. 4. Relative frequency of nonPD tensor estimates as a function of FA and SNR. The red lines denote the relative frequency of the nonPD LLS tensor estimates whereas the blue lines denote the relative frequency of the nonPD NLS tensor estimates. At each FA value and SNR level, 10000 simulated tensors were used in computing the relative frequencies.

$$\frac{\partial f(\boldsymbol{\beta}(\boldsymbol{\rho}))}{\partial \rho_l} = \sum_i \frac{\partial f(\boldsymbol{\beta})}{\partial \beta_i} \frac{\partial \beta_i}{\partial \rho_l} = 0 \quad [A2]$$

or

$$\begin{pmatrix} \frac{\partial \beta_1}{\partial \rho_1} & \dots & \frac{\partial \beta_m}{\partial \rho_1} \\ \vdots & \ddots & \vdots \\ \frac{\partial \beta_1}{\partial \rho_n} & \dots & \frac{\partial \beta_m}{\partial \rho_n} \end{pmatrix} \begin{pmatrix} \frac{\partial f(\boldsymbol{\beta})}{\partial \beta_1} \\ \vdots \\ \frac{\partial f(\boldsymbol{\beta})}{\partial \beta_m} \end{pmatrix} = \begin{pmatrix} 0 \\ \vdots \\ 0 \end{pmatrix}. \quad [A3]$$

The matrix above is known as the transpose of the Jacobian matrix. If the Jacobian matrix is invertible then the vector on the left-hand side of [A3] must be a zero vector. There-

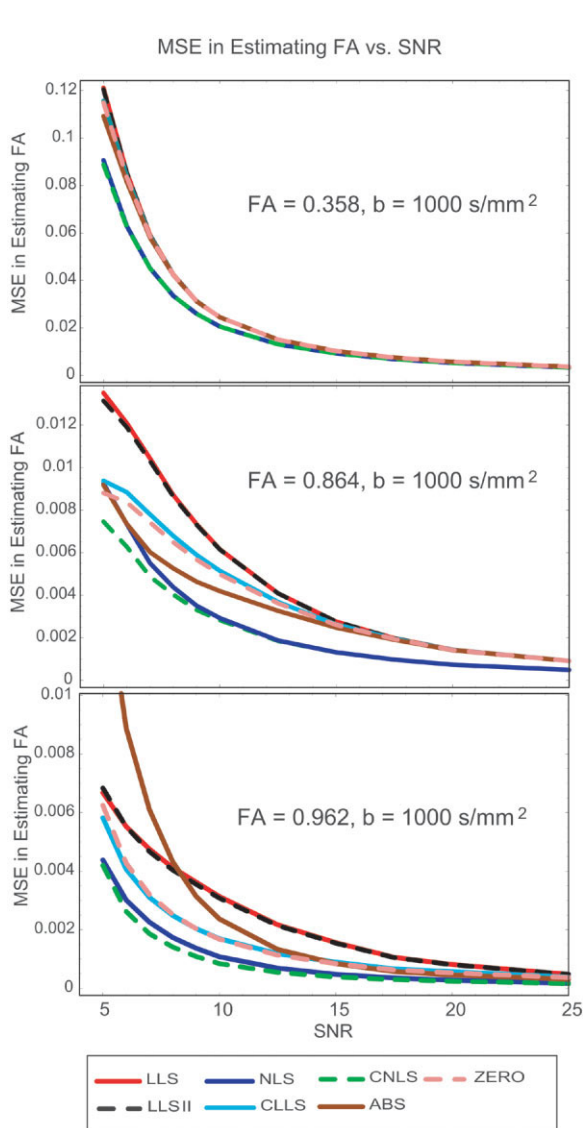


FIG. 5. Mean squared error in estimating FA as a function of SNR. Ten thousand simulated tensors were generated for the simulation at each FA value and SNR level. (Top) FA = 0.358, (middle) FA = 0.864, and (bottom) FA = 0.962. CNLS is uniformly better in terms of MSE than all other methods considered in this study.

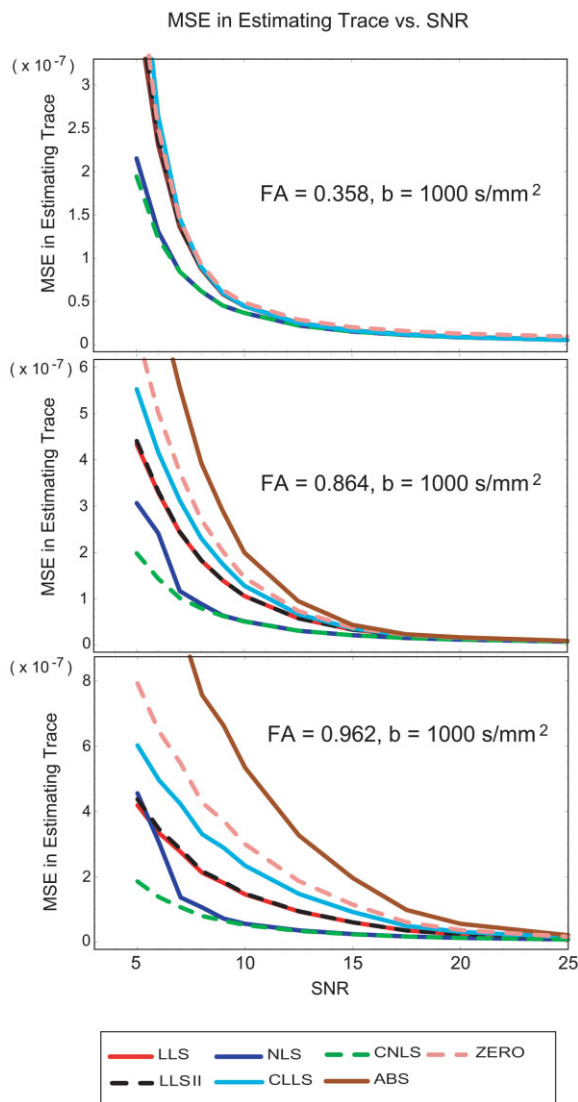


FIG. 6. Mean squared error in estimating trace as a function of SNR. Ten thousand simulated tensors were generated for each FA value and SNR level with the same trace. (Top) FA = 0.358, (middle) FA = 0.864, and (bottom) FA = 0.962. Again, CNLS is uniformly better in terms of MSE than all other methods considered in this study.

fore, this leads to the defining relation for the LLS method. That is,

$$\begin{pmatrix} \frac{\partial f(\boldsymbol{\beta})}{\partial \beta_1} \\ \vdots \\ \frac{\partial f(\boldsymbol{\beta})}{\partial \beta_m} \end{pmatrix} = \begin{pmatrix} 0 \\ \vdots \\ 0 \end{pmatrix}. \quad [\text{A4}]$$

For the specific mapping of $\boldsymbol{\beta}(\boldsymbol{\rho})$ in Eq. [10], the Jacobian matrix is a square matrix and its determinant is nonzero if R_0 , R_1 , and R_2 are nonzero. Specifically, the determinant of the Jacobian matrix is $8(R_0)^3(R_1)^2(R_2)^1$.

ACKNOWLEDGMENTS

The authors thank Dr. Richard Shrager, Dr. Carlo Pierpaoli, and Prof. Douglas Bates for helpful discussions. The authors also thank the reviewers for their insightful comments.

REFERENCES

1. Basser PJ, Mattiello J, LeBihan D. MR diffusion tensor and imaging. *Biophys J* 1994;66:259–267.
2. Basser PJ. Inferring microstructural features and the physiological state of tissues from diffusion-weighted images. *NMR Biomed* 1995;8:333–344.
3. Basser PJ, Pierpaoli C. Microstructural and physiological features of tissues elucidated by quantitative-diffusion-tensor MRI. *J Magn Reson B* 1996;111:209–219.
4. Mori S, Peter CM van Zijl. Fiber tracking: principles and strategies—a technical review. *NMR Biomed* 2002;15:468–480.
5. Conturo TE, McKinsty RC, Akbudak E, Robinson BH. Encoding of anisotropic diffusion with tetrahedral gradients: a general mathematical diffusion formalism and experimental results. *Magn Reson Med* 1996;35:399–412.
6. Pierpaoli C, Basser PJ. Toward a quantitative assessment of diffusion anisotropy. *Magn Reson Med* 1996;36:893–906.
7. Dong Q, Welsh RC, Chenevert TL, Carlos RC, Maly-Sundgren P, Gomez-Hassan DM, Mukherji SK. Clinical applications of diffusion tensor imaging. *J Magn Reson Imag* 2004;19:6–18.
8. Pinheiro JC, Bates DG. Unconstrained parametrizations for variance-covariance matrices. *Statist Comput* 1996;6:289–296.
9. Wang Z, Vemuri BC, Chen Y, Mareci TH. A Constrained variational principle for direct estimation and smoothing of the diffusion tensor field from complex DWI. *IEEE Trans Med Imaging* 2004;23:930–939.
10. Stejskal E, Tanner J. Spin diffusion measurements: spin echoes in the presence of a time-dependent field gradient. *J Chem Phys* 1965;42:288–292.
11. Bates DM, Watts DG. *Nonlinear regression analysis and its applications*. New York: Wiley; 1988. 34 p.
12. Golub GH, Van Loan CF. *Matrix computations*, 3rd ed. Baltimore: Johns Hopkins University Press; 1996. 143 p.
13. Anderson AW. Theoretical analysis of the effects of noise on diffusion tensor imaging. *Magn Reson Med* 2001;46:1174–1188.
14. Papadakis NG, Martin KM, Wilkinson ID, Huang CL. A measure of curve fitting error for noise filtering diffusion tensor MRI data. *J Magn Reson* 2003;164:1–9.
15. Mangin JF, Poupon C, Clark C, Le Bihan D, Bloch I. Distortion correction and robust tensor estimation for MR diffusion imaging. *Med Image Anal* 2002;6:191–198.
16. Chang LC, Jones DK, Pierpaoli C. RESTORE: Robust estimation of tensors by outlier rejection. *Magn Reson Med* 2005;53:1088–1095.
17. Horn RA, Johnson CR. *Matrix analysis*. New York: Cambridge University Press; 1985. p 402–407.
18. Press WH, Flannery BP, Teukolsky SA, Vetterling WT. *Numerical recipes in C*. New York: Cambridge University Press; 1992. 408 p.
19. Jones DK, Basser PJ. “Squashing peanuts and smashing pumpkins”: How noise distorts diffusion-weighted MR data. *Magn Reson Med* 2004;52:979–993.
20. Hasan KM, Basser PJ, Parker DL, Alexander AL. Analytical computation of the eigenvalues and eigenvectors in DT-MRI. *J Magn Reson* 2001;152:41–47.